

Improved Limits on Lepton-Flavor-Violating τ Decays to $\ell\phi$, $\ell\rho$, ℓK^* , and $\ell\bar{K}^*$

- B. Aubert,¹ Y. Karyotakis,¹ J. P. Lees,¹ V. Poireau,¹ E. Prencipe,¹ X. Prudent,¹ V. Tisserand,¹ J. Garra Tico,² E. Grauges,² M. Martinelli,^{3a,3b} A. Palano,^{3a,3b} M. Pappagallo,^{3a,3b} G. Eigen,⁴ B. Stugu,⁴ L. Sun,⁴ M. Battaglia,⁵ D. N. Brown,⁵ L. T. Kerth,⁵ Yu. G. Kolomensky,⁵ G. Lynch,⁵ I. L. Osipenkov,⁵ K. Tackmann,⁵ T. Tanabe,⁵ C. M. Hawkes,⁶ N. Soni,⁶ A. T. Watson,⁶ H. Koch,⁷ T. Schroeder,⁷ D. J. Asgeirsson,⁸ B. G. Fulsom,⁸ C. Hearty,⁸ T. S. Mattison,⁸ J. A. McKenna,⁸ M. Barrett,⁹ A. Khan,⁹ A. Randle-Conde,⁹ V. E. Blinov,^{10,*} A. R. Buzykaev,¹⁰ V. P. Druzhinin,¹⁰ V. B. Golubev,¹⁰ A. P. Onuchin,¹⁰ S. I. Serednyakov,¹⁰ Yu. I. Skovpen,¹⁰ E. P. Solodov,¹⁰ K. Yu. Todyshev,¹⁰ M. Bondioli,¹¹ S. Curry,¹¹ I. Eschrich,¹¹ D. Kirkby,¹¹ A. J. Lankford,¹¹ P. Lund,¹¹ M. Mandelkern,¹¹ E. C. Martin,¹¹ D. P. Stoker,¹¹ S. Abachi,¹² C. Buchanan,¹² H. Atmacan,¹³ J. W. Gary,¹³ F. Liu,¹³ O. Long,¹³ G. M. Vitug,¹³ Z. Yasin,¹³ L. Zhang,¹³ V. Sharma,¹⁴ C. Campagnari,¹⁵ T. M. Hong,¹⁵ D. Kovalskyi,¹⁵ M. A. Mazur,¹⁵ J. D. Richman,¹⁵ T. W. Beck,¹⁶ A. M. Eisner,¹⁶ C. A. Heusch,¹⁶ J. Kroeseberg,¹⁶ W. S. Lockman,¹⁶ A. J. Martinez,¹⁶ T. Schalk,¹⁶ B. A. Schumm,¹⁶ A. Seiden,¹⁶ L. O. Winstrom,¹⁶ C. H. Cheng,¹⁷ D. A. Doll,¹⁷ B. Echenard,¹⁷ F. Fang,¹⁷ D. G. Hitlin,¹⁷ I. Narsky,¹⁷ T. Piatenko,¹⁷ F. C. Porter,¹⁷ R. Andreassen,¹⁸ G. Mancinelli,¹⁸ B. T. Meadows,¹⁸ K. Mishra,¹⁸ M. D. Sokoloff,¹⁸ P. C. Bloom,¹⁹ W. T. Ford,¹⁹ A. Gaz,¹⁹ J. F. Hirschauer,¹⁹ M. Nagel,¹⁹ U. Nauenberg,¹⁹ J. G. Smith,¹⁹ S. R. Wagner,¹⁹ R. Ayad,^{20,†} A. Soffer,^{20,‡} W. H. Toki,²⁰ R. J. Wilson,²⁰ E. Feltresi,²¹ A. Hauke,²¹ H. Jasper,²¹ T. M. Karbach,²¹ J. Merkel,²¹ A. Petzold,²¹ B. Spaan,²¹ K. Wacker,²¹ M. J. Kobel,²² R. Nogowski,²² K. R. Schubert,²² R. Schwierz,²² A. Volk,²² D. Bernard,²³ G. R. Bonneaud,²³ E. Latour,²³ M. Verderi,²³ P. J. Clark,²⁴ S. Playfer,²⁴ J. E. Watson,²⁴ M. Andreotti,^{25a,25b} D. Bettoni,^{25a} C. Bozzi,^{25a} R. Calabrese,^{25a,25b} A. Cecchi,^{25a,25b} G. Cibinetto,^{25a,25b} E. Fioravanti,^{25a,25b} P. Franchini,^{25a,25b} E. Luppi,^{25a,25b} M. Munerato,^{25a,25b} M. Negrini,^{25a,25b} A. Petrella,^{25a,25b} L. Piemontese,^{25a} V. Santoro,^{25a,25b} R. Baldini-Ferroli,²⁶ A. Calcaterra,²⁶ R. de Sangro,²⁶ G. Finocchiaro,²⁶ S. Pacetti,²⁶ P. Patteri,²⁶ I. M. Peruzzi,^{26,§} M. Piccolo,²⁶ M. Rama,²⁶ A. Zallo,²⁶ R. Contri,^{27a,27b} E. Guido,^{27a} M. Lo Vetere,^{27a,27b} M. R. Monge,^{27a,27b} S. Passaggio,^{27a} C. Patrignani,^{27a,27b} E. Robutti,^{27a} S. Tosi,^{27a,27b} K. S. Chaisanguanthum,²⁸ M. Morii,²⁸ A. Adametz,²⁹ J. Marks,²⁹ S. Schenk,²⁹ U. Uwer,²⁹ F. U. Bernlochner,³⁰ V. Klose,³⁰ H. M. Lacker,³⁰ D. J. Bard,³¹ P. D. Dauncey,³¹ M. Tibbetts,³¹ P. K. Behera,³² M. J. Charles,³² U. Mallik,³² J. Cochran,³³ H. B. Crawley,³³ L. Dong,³³ V. Eyges,³³ W. T. Meyer,³³ S. Prell,³³ E. I. Rosenberg,³³ A. E. Rubin,³³ Y. Y. Gao,³⁴ A. V. Gritsan,³⁴ Z. J. Guo,³⁴ N. Arnaud,³⁵ J. Béquilleux,³⁵ A. D’Orazio,³⁵ M. Davier,³⁵ D. Derkach,³⁵ J. Firmino da Costa,³⁵ G. Grosdidier,³⁵ F. Le Diberder,³⁵ V. Lepeltier,³⁵ A. M. Lutz,³⁵ B. Malaescu,³⁵ S. Pruvot,³⁵ P. Roudeau,³⁵ M. H. Schune,³⁵ J. Serrano,³⁵ V. Sordini,^{35,||} A. Stocchi,³⁵ G. Wormser,³⁵ D. J. Lange,³⁶ D. M. Wright,³⁶ I. Bingham,³⁷ J. P. Burke,³⁷ C. A. Chavez,³⁷ J. R. Fry,³⁷ E. Gabathuler,³⁷ R. Gamet,³⁷ D. E. Hutchcroft,³⁷ D. J. Payne,³⁷ C. Touramanis,³⁷ A. J. Bevan,³⁸ C. K. Clarke,³⁸ F. Di Lodovico,³⁸ R. Sacco,³⁸ M. Sigamani,³⁸ G. Cowan,³⁹ S. Paramesvaran,³⁹ A. C. Wren,³⁹ D. N. Brown,⁴⁰ C. L. Davis,⁴⁰ A. G. Denig,⁴¹ M. Fritsch,⁴¹ W. Grndl,⁴¹ A. Hafner,⁴¹ K. E. Alwyn,⁴² D. Bailey,⁴² R. J. Barlow,⁴² G. Jackson,⁴² G. D. Lafferty,⁴² T. J. West,⁴² J. I. Yi,⁴² J. Anderson,⁴³ C. Chen,⁴³ A. Jawahery,⁴³ D. A. Roberts,⁴³ G. Simi,⁴³ J. M. Tuggle,⁴³ C. Dallapiccola,⁴⁴ E. Salvati,⁴⁴ S. Saremi,⁴⁴ R. Cowan,⁴⁵ D. Dujmic,⁴⁵ P. H. Fisher,⁴⁵ S. W. Henderson,⁴⁵ G. Sciolla,⁴⁵ M. Spitznagel,⁴⁵ R. K. Yamamoto,⁴⁵ M. Zhao,⁴⁵ P. M. Patel,⁴⁶ S. H. Robertson,⁴⁶ M. Schram,⁴⁶ A. Lazzaro,^{47a,47b} V. Lombardo,^{47a} F. Palombo,^{47a,47b} S. Stracka,^{47a,47b} J. M. Bauer,⁴⁸ L. Cremaldi,⁴⁸ R. Godang,^{48,¶} R. Kroeger,⁴⁸ D. J. Summers,⁴⁸ H. W. Zhao,⁴⁸ M. Simard,⁴⁹ P. Taras,⁴⁹ H. Nicholson,⁵⁰ G. De Nardo,^{51a,51b} L. Lista,^{51a} D. Monorchio,^{51a,51b} G. Onorato,^{51a,51b} C. Sciacca,^{51a,51b} G. Raven,⁵² H. L. Snoek,⁵² C. P. Jessop,⁵³ K. J. Knoepfel,⁵³ J. M. LoSecco,⁵³ W. F. Wang,⁵³ L. A. Corwin,⁵⁴ K. Honscheid,⁵⁴ H. Kagan,⁵⁴ R. Kass,⁵⁴ J. P. Morris,⁵⁴ A. M. Rahimi,⁵⁴ J. J. Regensburger,⁵⁴ S. J. Sekula,⁵⁴ Q. K. Wong,⁵⁴ N. L. Blount,⁵⁵ J. Brau,⁵⁵ R. Frey,⁵⁵ O. Ignokina,⁵⁵ J. A. Kolb,⁵⁵ M. Lu,⁵⁵ R. Rahmat,⁵⁵ N. B. Sinev,⁵⁵ D. Strom,⁵⁵ J. Strube,⁵⁵ E. Torrence,⁵⁵ G. Castelli,^{56a,56b} N. Gagliardi,^{56a,56b} M. Margoni,^{56a,56b} M. Morandin,^{56a} M. Posocco,^{56a} M. Rotondo,^{56a} F. Simonetto,^{56a,56b} R. Stroili,^{56a,56b} C. Voci,^{56a,56b} P. del Amo Sanchez,⁵⁷ E. Ben-Haim,⁵⁷ H. Briand,⁵⁷ J. Chauveau,⁵⁷ O. Hamon,⁵⁷ Ph. Leruste,⁵⁷ G. Marchiori,⁵⁷ J. Ocariz,⁵⁷ A. Perez,⁵⁷ J. Prendki,⁵⁷ S. Sitt,⁵⁷ L. Gladney,⁵⁸ M. Biasini,^{59a,59b} E. Manoni,^{59a,59b} C. Angelini,^{60a,60b} G. Batignani,^{60a,60b} S. Bettarini,^{60a,60b} G. Calderini,^{60a,60b,**} M. Carpinelli,^{60a,60b} A. Cervelli,^{60a,60b} F. Forti,^{60a,60b} M. A. Giorgi,^{60a,60b} A. Lusiani,^{60a,60c} M. Morganti,^{60a,60b} N. Neri,^{60a,60b} E. Paoloni,^{60a,60b} G. Rizzo,^{60a,60b} J. J. Walsh,^{60a} D. Lopes Pegna,⁶¹ C. Lu,⁶¹ J. Olsen,⁶¹ A. J. S. Smith,⁶¹ A. V. Telnov,⁶¹ F. Anulli,^{62a} E. Baracchini,^{62a,62b} G. Cavoto,^{62a} R. Faccini,^{62a,62b} F. Ferrarotto,^{62a} F. Ferroni,^{62a,62b} M. Gaspero,^{62a,62b} P. D. Jackson,^{62a} L. Li Gioi,^{62a} M. A. Mazzoni,^{62a} S. Morganti,^{62a} G. Piredda,^{62a} F. Renga,^{62a,62b} C. Voena,^{62a} M. Ebert,⁶³ T. Hartmann,⁶³ H. Schröder,⁶³ R. Waldi,⁶³ T. Adye,⁶⁴ B. Franek,⁶⁴ E. O. Olaiya,⁶⁴ F. F. Wilson,⁶⁴ S. Emery,⁶⁵ L. Esteve,⁶⁵ G. Hamel de Monchenault,⁶⁵ W. Kozanecki,⁶⁵ G. Vasseur,⁶⁵

Ch. Yèche,⁶⁵ M. Zito,⁶⁵ M. T. Allen,⁶⁶ D. Aston,⁶⁶ R. Bartoldus,⁶⁶ J. F. Benitez,⁶⁶ R. Cenci,⁶⁶ J. P. Coleman,⁶⁶ M. R. Convery,⁶⁶ J. C. Dingfelder,⁶⁶ J. Dorfan,⁶⁶ G. P. Dubois-Felsmann,⁶⁶ W. Dunwoodie,⁶⁶ R. C. Field,⁶⁶ A. M. Gabareen,⁶⁶ M. T. Graham,⁶⁶ P. Grenier,⁶⁶ C. Hast,⁶⁶ W. R. Innes,⁶⁶ J. Kaminski,⁶⁶ M. H. Kelsey,⁶⁶ H. Kim,⁶⁶ P. Kim,⁶⁶ M. L. Kocian,⁶⁶ D. W. G. S. Leith,⁶⁶ S. Li,⁶⁶ B. Lindquist,⁶⁶ S. Luitz,⁶⁶ V. Luth,⁶⁶ H. L. Lynch,⁶⁶ D. B. MacFarlane,⁶⁶ H. Marsiske,⁶⁶ R. Messner,^{66,*} D. R. Muller,⁶⁶ H. Neal,⁶⁶ S. Nelson,⁶⁶ C. P. O'Grady,⁶⁶ I. Ofte,⁶⁶ M. Perl,⁶⁶ B. N. Ratcliff,⁶⁶ A. Roodman,⁶⁶ A. A. Salnikov,⁶⁶ R. H. Schindler,⁶⁶ J. Schwiening,⁶⁶ A. Snyder,⁶⁶ D. Su,⁶⁶ M. K. Sullivan,⁶⁶ K. Suzuki,⁶⁶ S. K. Swain,⁶⁶ J. M. Thompson,⁶⁶ J. Va'vra,⁶⁶ A. P. Wagner,⁶⁶ M. Weaver,⁶⁶ C. A. West,⁶⁶ W. J. Wisniewski,⁶⁶ M. Wittgen,⁶⁶ D. H. Wright,⁶⁶ H. W. Wulsin,⁶⁶ A. K. Yarritu,⁶⁶ K. Yi,⁶⁶ C. C. Young,⁶⁶ V. Ziegler,⁶⁶ X. R. Chen,⁶⁷ H. Liu,⁶⁷ W. Park,⁶⁷ M. V. Purohit,⁶⁷ R. M. White,⁶⁷ J. R. Wilson,⁶⁷ P. R. Burchat,⁶⁸ A. J. Edwards,⁶⁸ T. S. Miyashita,⁶⁸ S. Ahmed,⁶⁹ M. S. Alam,⁶⁹ J. A. Ernst,⁶⁹ B. Pan,⁶⁹ M. A. Saeed,⁶⁹ S. B. Zain,⁶⁹ S. M. Spanier,⁷⁰ B. J. Wogsland,⁷⁰ R. Eckmann,⁷⁰ J. L. Ritchie,⁷⁰ A. M. Ruland,⁷¹ C. J. Schilling,⁷¹ R. F. Schwitters,⁷¹ B. C. Wray,⁷¹ B. W. Drummond,⁷² J. M. Izen,⁷² X. C. Lou,⁷² F. Bianchi,^{73a,73b} D. Gamba,^{73a,73b} M. Pelliccioni,^{73a,73b} M. Bomben,^{74a,74b} L. Bosisio,^{47a,47b} C. Cartaro,^{47a,47b} G. Della Ricca,^{47a,47b} L. Lanceri,^{47a,47b} L. Vitale,^{47a,47b} V. Azzolini,⁷⁵ N. Lopez-March,⁷⁵ F. Martinez-Vidal,⁷⁵ D. A. Milanes,⁷⁵ A. Oyanguren,⁷⁵ J. Albert,⁷⁶ Sw. Banerjee,⁷⁶ B. Bhuyan,⁷⁶ H. H. F. Choi,⁷⁶ K. Hamano,⁷⁶ G. J. King,⁷⁶ R. Kowalewski,⁷⁶ M. J. Lewczuk,⁷⁶ I. M. Nugent,⁷⁶ J. M. Roney,⁷⁶ R. J. Sobie,⁷⁶ T. J. Gershon,⁷⁷ P. F. Harrison,⁷⁷ J. Ilic,⁷⁷ T. E. Latham,⁷⁷ G. B. Mohanty,⁷⁷ E. M. T. Puccio,⁷⁷ H. R. Band,⁷⁸ X. Chen,⁷⁸ S. Dasu,⁷⁸ K. T. Flood,⁷⁸ Y. Pan,⁷⁸ R. Prepost,⁷⁸ C. O. Vuosalo,⁷⁸ and S. L. Wu⁷⁸

(BABAR Collaboration)

¹Laboratoire d'Annecy-le-Vieux de Physique des Particules (LAPP), Université de Savoie, CNRS/IN2P3, F-74941 Annecy-Le-Vieux, France

²Universitat de Barcelona, Facultat de Fisica, Departament ECM, E-08028 Barcelona, Spain

^{3a}INFN Sezione di Bari, I-70126 Bari, Italy

^{3b}Dipartimento di Fisica, Università di Bari, I-70126 Bari, Italy

⁴University of Bergen, Institute of Physics, N-5007 Bergen, Norway

⁵Lawrence Berkeley National Laboratory and University of California, Berkeley, California 94720, USA

⁶University of Birmingham, Birmingham, B15 2TT, United Kingdom

⁷Ruhr Universität Bochum, Institut für Experimentalphysik 1, D-44780 Bochum, Germany

⁸University of British Columbia, Vancouver, British Columbia, Canada V6T 1Z1

⁹Brunel University, Uxbridge, Middlesex UB8 3PH, United Kingdom

¹⁰Budker Institute of Nuclear Physics, Novosibirsk 630090, Russia

¹¹University of California at Irvine, Irvine, California 92697, USA

¹²University of California at Los Angeles, Los Angeles, California 90024, USA

¹³University of California at Riverside, Riverside, California 92521, USA

¹⁴University of California at San Diego, La Jolla, California 92093, USA

¹⁵University of California at Santa Barbara, Santa Barbara, California 93106, USA

¹⁶University of California at Santa Cruz, Institute for Particle Physics, Santa Cruz, California 95064, USA

¹⁷California Institute of Technology, Pasadena, California 91125, USA

¹⁸University of Cincinnati, Cincinnati, Ohio 45221, USA

¹⁹University of Colorado, Boulder, Colorado 80309, USA

²⁰Colorado State University, Fort Collins, Colorado 80523, USA

²¹Technische Universität Dortmund, Fakultät Physik, D-44221 Dortmund, Germany

²²Technische Universität Dresden, Institut für Kern- und Teilchenphysik, D-01062 Dresden, Germany

²³Laboratoire Leprince-Ringuet, CNRS/IN2P3, Ecole Polytechnique, F-91128 Palaiseau, France

²⁴University of Edinburgh, Edinburgh EH9 3JZ, United Kingdom

^{25a}INFN Sezione di Ferrara, I-44100 Ferrara, Italy

^{25b}Dipartimento di Fisica, Università di Ferrara, I-44100 Ferrara, Italy

²⁶INFN Laboratori Nazionali di Frascati, I-00044 Frascati, Italy

^{27a}INFN Sezione di Genova, I-16146 Genova, Italy

^{27b}Dipartimento di Fisica, Università di Genova, I-16146 Genova, Italy

²⁸Harvard University, Cambridge, Massachusetts 02138, USA

²⁹Universität Heidelberg, Physikalisches Institut, Philosophenweg 12, D-69120 Heidelberg, Germany

³⁰Humboldt-Universität zu Berlin, Institut für Physik, Newtonstr. 15, D-12489 Berlin, Germany

³¹Imperial College London, London, SW7 2AZ, United Kingdom

³²University of Iowa, Iowa City, Iowa 52242, USA

³³Iowa State University, Ames, Iowa 50011-3160, USA

- ³⁴*Johns Hopkins University, Baltimore, Maryland 21218, USA*
- ³⁵*Laboratoire de l'Accélérateur Linéaire, IN2P3/CNRS et Université Paris-Sud 11, Centre Scientifique d'Orsay, B. P. 34, F-91898 Orsay Cedex, France*
- ³⁶*Lawrence Livermore National Laboratory, Livermore, California 94550, USA*
- ³⁷*University of Liverpool, Liverpool L69 7ZE, United Kingdom*
- ³⁸*Queen Mary, University of London, London, E1 4NS, United Kingdom*
- ³⁹*University of London, Royal Holloway and Bedford New College, Egham, Surrey TW20 0EX, United Kingdom*
- ⁴⁰*University of Louisville, Louisville, Kentucky 40292, USA*
- ⁴¹*Johannes Gutenberg-Universität Mainz, Institut für Kernphysik, D-55099 Mainz, Germany*
- ⁴²*University of Manchester, Manchester M13 9PL, United Kingdom*
- ⁴³*University of Maryland, College Park, Maryland 20742, USA*
- ⁴⁴*University of Massachusetts, Amherst, Massachusetts 01003, USA*
- ⁴⁵*Massachusetts Institute of Technology, Laboratory for Nuclear Science, Cambridge, Massachusetts 02139, USA*
- ⁴⁶*McGill University, Montréal, Québec, Canada H3A 2T8*
- ^{47a}*INFN Sezione di Milano, I-20133 Milano, Italy*
- ^{47b}*Dipartimento di Fisica, Università di Milano, I-20133 Milano, Italy*
- ⁴⁸*University of Mississippi, University, Mississippi 38677, USA*
- ⁴⁹*Université de Montréal, Physique des Particules, Montréal, Québec, Canada H3C 3J7*
- ⁵⁰*Mount Holyoke College, South Hadley, Massachusetts 01075, USA*
- ^{51a}*INFN Sezione di Napoli, I-80126 Napoli, Italy*
- ^{51b}*Dipartimento di Scienze Fisiche, Università di Napoli Federico II, I-80126 Napoli, Italy*
- ⁵²*NIKHEF, National Institute for Nuclear Physics and High Energy Physics, NL-1009 DB Amsterdam, The Netherlands*
- ⁵³*University of Notre Dame, Notre Dame, Indiana 46556, USA*
- ⁵⁴*Ohio State University, Columbus, Ohio 43210, USA*
- ⁵⁵*University of Oregon, Eugene, Oregon 97403, USA*
- ^{56a}*INFN Sezione di Padova, I-35131 Padova, Italy*
- ^{56b}*Dipartimento di Fisica, Università di Padova, I-35131 Padova, Italy*
- ⁵⁷*Laboratoire de Physique Nucléaire et de Hautes Energies, IN2P3/CNRS, Université Pierre et Marie Curie-Paris6, Université Denis Diderot-Paris7, F-75252 Paris, France*
- ⁵⁸*University of Pennsylvania, Philadelphia, Pennsylvania 19104, USA*
- ^{59a}*INFN Sezione di Perugia, I-06100 Perugia, Italy*
- ^{59b}*Dipartimento di Fisica, Università di Perugia, I-06100 Perugia, Italy*
- ^{60a}*INFN Sezione di Pisa, I-56127 Pisa, Italy*
- ^{60b}*Dipartimento di Fisica, Università di Pisa, I-56127 Pisa, Italy*
- ^{60c}*Scuola Normale Superiore di Pisa, I-56127 Pisa, Italy*
- ⁶¹*Princeton University, Princeton, New Jersey 08544, USA*
- ^{62a}*INFN Sezione di Roma, I-00185 Roma, Italy*
- ^{62b}*Dipartimento di Fisica, Università di Roma La Sapienza, I-00185 Roma, Italy*
- ⁶³*Universität Rostock, D-18051 Rostock, Germany*
- ⁶⁴*Rutherford Appleton Laboratory, Chilton, Didcot, Oxon, OX11 0QX, United Kingdom*
- ⁶⁵*CEA, Ifju, SPP, Centre de Saclay, F-91191 Gif-sur-Yvette, France*
- ⁶⁶*SLAC National Accelerator Laboratory, Stanford, California 94309 USA*
- ⁶⁷*University of South Carolina, Columbia, South Carolina 29208, USA*
- ⁶⁸*Stanford University, Stanford, California 94305-4060, USA*
- ⁶⁹*State University of New York, Albany, New York 12222, USA*
- ⁷⁰*University of Tennessee, Knoxville, Tennessee 37996, USA*
- ⁷¹*University of Texas at Austin, Austin, Texas 78712, USA*
- ⁷²*University of Texas at Dallas, Richardson, Texas 75083, USA*
- ^{73a}*INFN Sezione di Torino, I-10125 Torino, Italy*
- ^{73b}*Dipartimento di Fisica Sperimentale, Università di Torino, I-10125 Torino, Italy*
- ^{74a}*INFN Sezione di Trieste, I-34127 Trieste, Italy*
- ^{74b}*Dipartimento di Fisica, Università di Trieste, I-34127 Trieste, Italy*
- ⁷⁵*IFIC, Universitat de Valencia-CSIC, E-46071 Valencia, Spain*
- ⁷⁶*University of Victoria, Victoria, British Columbia, Canada V8W 3P6*
- ⁷⁷*Department of Physics, University of Warwick, Coventry CV4 7AL, United Kingdom*
- ⁷⁸*University of Wisconsin, Madison, Wisconsin 53706, USA*

(Received 2 April 2009; published 10 July 2009)

We search for the neutrinoless, lepton-flavor-violating tau decays $\tau^- \rightarrow \ell^- V^0$, where ℓ is an electron or muon and V^0 is a vector meson reconstructed as $\phi \rightarrow K^+ K^-, \rho \rightarrow \pi^+ \pi^-, K^* \rightarrow K^+ \pi^-, \bar{K}^* \rightarrow K^- \pi^+$. The analysis has been performed using 451 fb^{-1} of data collected at an $e^+ e^-$ center-of-mass energy near

10.58 GeV with the *BABAR* detector at the PEP-II storage rings. The number of events found in the data is compatible with the background expectation, and upper limits on the branching fractions are set in the range $(2.6\text{--}19) \times 10^{-8}$ at the 90% confidence level.

DOI: 10.1103/PhysRevLett.103.021801

PACS numbers: 13.35.Dx, 14.60.Fg, 11.30.Hv

Lepton-flavor violation (LFV) involving tau leptons has never been observed, and recent experimental results have placed stringent limits on the branching fractions for two- and three-body neutrinoless tau decays [1–3]. Many descriptions of physics beyond the standard model (SM) predict such decays [4,5]; and certain models [6,7] specifically predict semileptonic tau decays such as $\tau \rightarrow \ell \phi$, $\ell \rho$, ℓK^* , $\ell \bar{K}^*$ ($\tau^- \rightarrow \ell^- V^0$), with rates as high as the current experimental limits [3]. An observation of these decays would be a clear signature of physics beyond the SM, while improved limits will further constrain models of new physics.

This Letter presents a search for LFV in a set of eight neutrinoless decay modes $\tau^- \rightarrow \ell^- V^0$ [8], where ℓ is an electron or muon and V^0 is a neutral vector meson decaying to two charged hadrons ($V^0 \rightarrow h^+ h^-$) via one of the following four decay modes: $\phi \rightarrow K^+ K^-$, $\rho \rightarrow \pi^+ \pi^-$, $K^* \rightarrow K^+ \pi^-$, $K^* \rightarrow \pi^+ K^-$. This analysis is based on data recorded by the *BABAR* detector at the PEP-II asymmetric-energy $e^+ e^-$ storage rings operated at the SLAC National Accelerator Laboratory. The *BABAR* detector is described in detail in Ref. [9]. The data sample consists of 410 fb^{-1} recorded at an $e^+ e^-$ center-of-mass (c.m.) energy $\sqrt{s} = 10.58 \text{ GeV}$, and 40.8 fb^{-1} recorded at $\sqrt{s} = 10.54 \text{ GeV}$. With a calculated cross section for tau pairs of $\sigma_{\tau\tau} = 0.919 \pm 0.003 \text{ nb}$ [10,11] at the stated luminosity-weighted \sqrt{s} , this data set corresponds to the production of about 830×10^6 tau decays.

We use a Monte Carlo (MC) simulation of lepton-flavor-violating tau decays to optimize the search. Tau-pair events including higher-order radiative corrections are generated using KK2F [11]. One tau decays via two-body phase space to a lepton and a vector meson, with the meson decaying according to the measured branching fractions [12]. The other tau decays via SM processes simulated with TAUOLA [13]. Final-state radiative effects are simulated for all decays using PHOTOS [14]. The detector response is modeled with GEANT4 [15], and the simulated events are then reconstructed in the same manner as data. SM background processes are modeled with a similar software framework.

We search for the signal decay $\tau^- \rightarrow \ell^- V^0 \rightarrow \ell^- h^+ h^-$ by reconstructing $e^+ e^- \rightarrow \tau^+ \tau^-$ candidates in which three charged particles, each identified as the appropriate lepton or hadron, have an invariant mass and energy close to that of the parent tau lepton. Candidate signal events are first required to have a “3-1 topology”, where one tau decay yields three charged particles, while the second tau decay yields one charged particle. This requirement on the second tau decay greatly reduces the background from con-

tinuum multihadron events. Events with four well-reconstructed tracks and zero net charge are selected, and the tracks are required to point toward a common region consistent with $\tau^+ \tau^-$ production and decay. The polar angle of all four tracks in the laboratory frame is required to be within the calorimeter acceptance. Pairs of oppositely charged tracks are ignored if their invariant mass, assuming electron mass hypotheses, is less than $30 \text{ MeV}/c^2$. Such tracks are likely to be from photon conversions in the traversed material. The event is divided into hemispheres in the $e^+ e^-$ c.m. frame using the plane perpendicular to the thrust axis, as calculated from the observed tracks and neutral energy deposits. The signal (three-prong) hemisphere must contain exactly three tracks while the other (one-prong) hemisphere must contain exactly one. Each of the charged particles found in the three-prong hemisphere must be identified as a lepton or hadron candidate appropriate to the search channel. The relevant particle identification capabilities of the *BABAR* detector are described in Ref. [2].

To further suppress backgrounds from quark pair production, Bhabha scattering events, and SM tau-pair production, we apply additional selection criteria separately in the eight different search channels. Specific cut values are shown in Table I. All selection criteria are optimized to provide the smallest expected upper limit on the branching fraction in the background-only hypothesis. Resonant decays are selected with cuts on the invariant mass of the two hadrons in the three-prong hemisphere (m_{hh}). The invariant mass of the one-prong hemisphere ($m_{1\text{ pr}}$) is calculated from the charged and neutral particles in that hemisphere and the total missing momentum in the event. As the missing momentum in signal events results from one or

TABLE I. Values of the cuts on the selection variables described in the text. Masses are in units of GeV/c^2 , and momenta in units of GeV/c .

Channel	$e\phi$	$\mu\phi$	$e\rho$	$\mu\rho$	eK^*	μK^*	$e\bar{K}^*$	$\mu\bar{K}^*$
m_{hh} min	1.000	1.005	0.6	0.6	0.8	0.82	0.80	0.78
m_{hh} max	1.040	1.035	0.92	0.96	1.0	0.98	1.04	1.00
$m_{1\text{ pr}}$ min	0.3	0.4	0.3	0.3	0.3	0.2	0.3	...
$m_{1\text{ pr}}$ max	2.5	2.5	2.5	2.5	2.5	2.5	2.5	...
p_T^{miss} min	0.4	0.3	0.4	0.4	0.4	0.4	0.4	0.4
$p_T^{\text{c.m.s}}$ min	0.5	0.6	...	0.3	...
n_1^γ pr max	4	3	3	1	...	3	...	2
n_3^γ pr max	3	1	2	1	...	2	...	1

more neutrinos in the one-prong hemisphere, this mass is required to be near the tau mass. Background events from quark pair production are suppressed with cuts on the missing transverse momentum in the event (p_T^{miss}), the scalar sum of all transverse momenta in the c.m. frame ($p_{\text{T}}^{\text{c.m.},s}$), and the number of photons in the one-prong (1 pr) and three-prong (3 pr) hemispheres (n_1^{γ} , n_3^{γ}). To reduce the background contribution from radiative Bhabha and dimuon events, the one-prong and three-prong momentum vectors must not be collinear in the c.m. frame. For the same reason, the one-prong track must not be identified as an electron for the $\tau^- \rightarrow e^- \rho$ search.

As a final discriminant, we require candidate signal events to have an invariant mass and total energy in the three-prong hemisphere consistent with a parent tau lepton. These quantities are calculated from the measured track momenta, assuming lepton and hadron masses that correspond to the neutrinoless tau decay in each search channel. The energy difference is defined as $\Delta E \equiv E_{\text{rec}}^* - E_{\text{beam}}^*$, where E_{rec}^* is the total energy of the tracks observed in the three-prong hemisphere and E_{beam}^* is the beam energy, with both quantities calculated in the c.m. frame. The mass difference is defined as $\Delta M \equiv M_{\text{EC}} - m_\tau$ where M_{EC} is calculated from a kinematic fit to the three-prong track momenta with the energy constrained to be $\sqrt{s}/2$ in the c.m. frame, and $m_\tau = 1.777 \text{ GeV}/c^2$ is the tau mass [12]. While the energy constraint significantly reduces the spread of ΔM values, it also introduces a correlation between ΔM and ΔE , which must be taken into account when fitting distributions in this two-dimensional space.

Detector resolution and radiative effects broaden the signal distributions in the $(\Delta M, \Delta E)$ plane. Because of the correlation between ΔM and ΔE , the radiation of

photons from the incoming e^+e^- particles produces a tail at positive values of ΔM and negative values of ΔE . Radiation from the final-state leptons, which is more likely for electrons than muons, leads to a tail at low values of ΔE . Rectangular signal boxes (SB) in the $(\Delta M, \Delta E)$ plane are defined separately for each search channel. As with previous selection criteria, the SB boundaries are chosen to provide the smallest expected upper limit on the branching fraction. The expected upper limit is estimated using only MC simulations and data events in the sideband region, as described below. Figure 1 shows the observed data in the large box (LB) of the $(\Delta M, \Delta E)$ plane, along with the SB boundaries and the expected signal distributions. Table II lists the channel-specific dimensions of the SB. While a small fraction of the signal events lie outside the SB, the effect on the final result is negligible. To avoid bias, we use a blinded analysis procedure with the number of data events in the SB remaining unknown until the selection criteria are finalized and all cross-checks are performed.

There are three main classes of background events remaining after the selection criteria are applied: charm quark production ($c\bar{c}$), low-multiplicity continuum $e^+e^- \rightarrow u\bar{u}/d\bar{d}/s\bar{s}$ events (uds), and SM $\tau^+\tau^-$ pair events. The background from two-photon production is negligible. These three background classes have distinctive distributions in the $(\Delta M, \Delta E)$ plane. The uds events tend to populate the plane evenly, with a fall-off at positive values of ΔE . Events in the $c\bar{c}$ sample exhibit peaks at positive values of ΔM due to D and D_s mesons, and are generally restricted to negative values of ΔE . The $\tau^+\tau^-$ background events are restricted to negative values of both ΔE and ΔM .

The expected background rates in the SB are determined by fitting a set of two-dimensional probability density

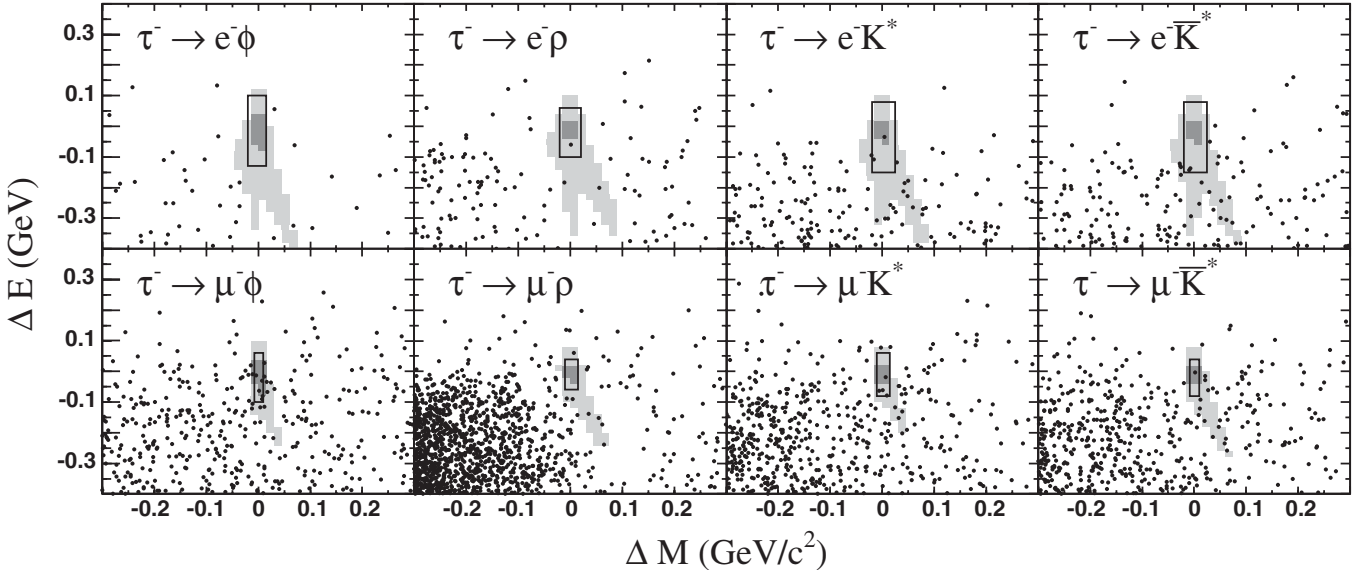


FIG. 1. Observed data shown as dots in the large box of the $(\Delta M, \Delta E)$ plane and the boundaries of the signal box. The dark and light shading indicates contours containing 50% and 90% of the selected MC signal events, respectively.

TABLE II. Signal Box boundaries; ΔM is in units of GeV/c^2 and ΔE in units of GeV .

Mode	$e\phi$	$e\rho$	eK^*	$e\bar{K}^*$	$\mu\phi$	$\mu\rho$	μK^*	$\mu\bar{K}^*$
ΔM_{\min}	-0.02	-0.02	-0.02	-0.015	-0.008	-0.01	-0.01	-0.008
ΔM_{\max}	0.015	0.02	0.02	0.02	0.01	0.015	0.01	0.01
ΔE_{\min}	-0.13	-0.10	-0.15	-0.125	-0.09	-0.06	-0.08	-0.08
ΔE_{\max}	0.10	0.06	0.08	0.06	0.06	0.04	0.04	0.06

functions (PDFs) to the observed data in the grand sideband (GS) region of the $(\Delta M, \Delta E)$ plane. The GS region is defined as the LB minus the SB. The shapes of the PDFs are determined by fits to the $(\Delta M, \Delta E)$ distributions of background MC samples in the LB, as described in Ref. [1]. The present analysis makes use of the same parameterization as Ref. [1] for the ΔE spectra, except for the case of the $c\bar{c}$ spectrum in some search channels. In these cases, combinations of polynomial and Gaussian functions are used. The choice of PDF for the ΔM spectrum of the uds samples is the same as used in Ref. [1], while the $\tau^+\tau^-$ and $c\bar{c}$ ΔM spectra are modeled with Gaussian and polynomial functions, or the Crystal Ball function [16]. All shape parameters, including a rotation angle accounting for the correlation between ΔE and ΔM , are determined from the fits to MC samples.

Once the shapes of the three background PDFs are determined, an unbinned extended maximum likelihood fit to the data in the GS region is used to find the expected background count in the SB. The fits to the background MC samples and to data are performed separately for each of the eight search channels.

We estimate the signal event selection efficiency with a MC simulation of lepton-flavor violating tau decays. Between 20% and 40% of the MC signal events pass the 3-1 topology requirement. The efficiency for identification of the three final-state particles ranges from 42% for $\tau^- \rightarrow \mu^- K^*$ to 82% for $\tau^- \rightarrow e^- \rho$. The total efficiency for signal events to be found in the SB is shown in Table III, and ranges from 4.1% to 8.0%. This efficiency includes the branching fraction for the vector meson decay to charged daughters, as well as the branching fraction for one-prong tau decays.

The particle identification efficiencies and misidentification probabilities have been measured with control samples both for data and MC events, as a function of particle momentum, polar angle, and azimuthal angle in the laboratory frame. The systematic uncertainties related to the particle identification have been estimated from the statistical uncertainty of the efficiency measurements and from the difference between data and MC efficiencies. These uncertainties range from 1.7% for $\tau^- \rightarrow e^- \rho$ to 9.0% for $\tau^- \rightarrow \mu^- \rho$ [17]. The modeling of the tracking efficiency and the uncertainty from the one-prong tau branching fraction each contribute an additional 1% uncertainty. Furthermore, the uncertainty on the intermediate branching fractions $\mathcal{B}(\phi, K^*, \bar{K}^* \rightarrow h^+ h^-)$ contributes a

1% uncertainty. All other sources of uncertainty in the signal efficiency are found to be negligible, including the statistical limitations of the MC signal samples, modeling of radiative effects by the generator, track momentum resolution, trigger performance, and the choice of observables used for event selection.

Since the background levels are extracted directly from the data, systematic uncertainties on the background estimation are directly related to the background parameterization and the fit technique used. Uncertainties related to the fits to the background samples are estimated by varying the background shape parameters according to the covariance matrix and repeating the fits, and range from 3.8% to 10%. Uncertainties related to the fits for the background yields in the GS are estimated by varying the yields within their errors, and range from 4.1% to 16%. The total uncertainty on the background estimates is shown in Table III. Cross-checks of the background estimation are performed by comparing the number of events expected and observed in sideband regions immediately neighboring the SB for each search channel. No major discrepancies are observed.

The number of events observed (N_{obs}) and the number of background events expected (N_{bgd}) are shown in Table III. The POLE calculator [18], based on the method of Feldman and Cousins [19], is used to place 90% CL upper limits on the number of signal events (N_{UL}^{90}), which include uncertainties on N_{bgd} and on the selection efficiency (ε). For the $\tau^- \rightarrow \mu^- \phi$ search, the POLE calculation results in a two-sided interval at 90% CL for the number of signal

TABLE III. Efficiency estimate, number of expected background events (N_{bgd}), number of observed events (N_{obs}), observed upper limit at 90% C.L. on the number of signal events (N_{UL}^{90}), expected branching fraction upper limit at 90% C.L. ($\mathcal{B}_{\text{exp}}^{90}$), and observed branching fraction upper limit at 90% C.L. ($\mathcal{B}_{\text{UL}}^{90}$). $\mathcal{B}_{\text{exp}}^{90}$ and $\mathcal{B}_{\text{UL}}^{90}$ are in units of 10^{-8} .

Mode	$\varepsilon[\%]$	N_{bgd}	N_{obs}	N_{UL}^{90}	$\mathcal{B}_{\text{exp}}^{90}$	$\mathcal{B}_{\text{UL}}^{90}$
$e\phi$	6.43 ± 0.16	0.68 ± 0.12	0	1.8	5.0	3.1
$\mu\phi$	5.18 ± 0.27	2.76 ± 0.16	6	8.7	8.2	19
$e\rho$	7.31 ± 0.18	1.32 ± 0.17	1	3.1	4.9	4.6
$\mu\rho$	4.52 ± 0.41	2.04 ± 0.19	0	1.1	8.9	2.6
eK^*	8.00 ± 0.19	1.65 ± 0.23	2	4.3	4.8	5.9
μK^*	4.57 ± 0.36	1.79 ± 0.21	4	7.1	8.5	17
$e\bar{K}^*$	7.76 ± 0.18	2.76 ± 0.28	2	3.2	5.4	4.6
$\mu\bar{K}^*$	4.11 ± 0.32	1.72 ± 0.17	1	2.7	9.3	7.3

events: [0.39–8.65]. Upper limits on the branching fractions are calculated according to $\mathcal{B}_{\text{UL}}^{90} = N_{\text{UL}}^{90}/(2\epsilon \mathcal{L}\sigma_{\tau\tau})$, where the values \mathcal{L} and $\sigma_{\tau\tau}$ are the integrated luminosity and $\tau^+\tau^-$ cross section, respectively. The uncertainty on the product $\mathcal{L}\sigma_{\tau\tau}$ is 1.0%. Table III lists the upper limits on the branching fractions, as well as the expected upper limit $\mathcal{B}_{\text{exp}}^{90}$, defined as the mean upper limit expected in the background-only hypothesis. The 90% CL upper limits on the $\tau \rightarrow \ell\phi$, $\ell\rho$, ℓK^* , $\ell\bar{K}^*$ branching fractions are in the range $(2.6\text{--}19) \times 10^{-8}$, and these limits represent improvements over the previous experimental bounds [3] in almost all search channels.

We are grateful for the excellent luminosity and machine conditions provided by our PEP-II colleagues, and for the substantial dedicated effort from the computing organizations that support *BABAR*. The collaborating institutions wish to thank SLAC for its support and kind hospitality. This work is supported by DOE and NSF (USA), NSERC (Canada), CEA and CNRS-IN2P3 (France), BMBF and DFG (Germany), INFN (Italy), FOM (The Netherlands), NFR (Norway), MES (Russia), MEC (Spain), and STFC (United Kingdom). Individuals have received support from the Marie Curie EIF (European Union) and the A. P. Sloan Foundation.

*Deceased.

[†]Present address: Temple University, Philadelphia, PA 19122, USA.

[‡]Present address: Tel Aviv University, Tel Aviv, 69978, Israel.

[§]Also with Università di Perugia, Dipartimento di Fisica, Perugia, Italy.

^{||}Also with Università di Roma La Sapienza, I-00185 Roma, Italy.

[¶]Now at University of South Alabama, Mobile, AL 36688, USA.

^{**}Also with Laboratoire de Physique Nucléaire et de Hautes Energies, IN2P3/CNRS, Université Pierre et Marie Curie-Paris6, Université Denis Diderot-Paris7, F-75252 Paris, France.

^{††}Also with Università di Sassari, Sassari, Italy.

- [1] B. Aubert *et al.* (*BABAR* Collaboration), Phys. Rev. Lett. **99**, 251803 (2007).
- [2] B. Aubert *et al.* (*BABAR* Collaboration), Phys. Rev. Lett. **95**, 191801 (2005).
- [3] Y. Nishio *et al.* (*Belle* Collaboration), Phys. Lett. B **664**, 35 (2008).
- [4] P. Paradisi, J. High Energy Phys. 10 (2005) 006.
- [5] A. Brignole and A. Rossi, Phys. Lett. B **566**, 217 (2003).
- [6] A. Brignole and A. Rossi, Nucl. Phys. **B701**, 3 (2004).
- [7] E. Arganda, J. M. Herrero, and J. Portoles, J. High Energy Phys. 06 (2008) 079.
- [8] Throughout this Letter, charge conjugate decay modes are implied.
- [9] B. Aubert *et al.* (*BABAR* Collaboration), Nucl. Instrum. Methods Phys. Res., Sect. A **479**, 1 (2002).
- [10] S. Banerjee *et al.*, Phys. Rev. D **77**, 054021 (2008).
- [11] S. Jadach, B. F. L. Ward, and Z. Wąs, Comput. Phys. Commun. **130**, 260 (2000).
- [12] Y.-M. Yao *et al.* (Particle Data Group), J. Phys. G **33**, 1 (2006).
- [13] S. Jadach *et al.*, Comput. Phys. Commun. **76**, 361 (1993).
- [14] E. Barberio and Z. Wąs, Comput. Phys. Commun. **79**, 291 (1994).
- [15] S. Agostinelli *et al.* (GEANT4 Collaboration), Nucl. Instrum. Methods Phys. Res., Sect. A **506**, 250 (2003).
- [16] M. J. Oreglia, Ph.D. thesis [SLAC-236, 1980, Appendix D]; J. E. Gaiser, Ph.D. thesis [SLAC-255, 1982, Appendix F]; T. Skwarnicki, Ph.D. thesis [DESY F31-86-02, 1986, Appendix E].
- [17] All uncertainties quoted in the text are relative.
- [18] J. Conrad *et al.*, Phys. Rev. D **67**, 012002 (2003).
- [19] G. J. Feldman and R. D. Cousins, Phys. Rev. D **57**, 3873 (1998).